

A model for coexisting antiferromagnetism and superconductivity

Edwin Langmann^a, Jack Lidmar^a, Manfred Salmhofer^b, and Mats Wallin^a

^a *Theoretical Physics, Royal Institute of Technology, S-100 44 Stockholm, Sweden*

^b *Mathematik, ETH Zentrum, 8092 Zürich, Switzerland*

(December 2, 2024)

We consider a lattice fermion model which describes coexisting antiferromagnetism and superconductivity (SC) with the latter resulting from a weak pairing interaction. We argue that this model gives a simple effective description of the effect of antiferromagnetic correlations on SC in doped Hubbard-like models and thus is an effective model for high temperature superconductors. We also argue that this model can be derived from a variant of the periodic Anderson model for heavy fermions. We use a flexible path integral formalism which allows to derive mean field equations for this model efficiently. Our formalism can be easily adapted to other models, and it is also a convenient starting point to derive fluctuation corrections to mean field theory. We then analyze the mean field Eqs. for the two dimensional version of this model. Evaluating the SC critical temperature and the temperature dependence of the SC gap, we find that SC can be significantly enhanced by antiferromagnetism. This effect is largest in case of nearest neighbor attraction, and we find that the most stable channel usually is a $d_{x^2-y^2}$ -wave gap. We also give a simple physical explanation of the results of our systematic stability analysis.

PACS numbers: 21.60.Jz, 74.72.-h, 74.70.Tx

I. INTRODUCTION

Motivated by heavy-fermion- and high-temperature superconductors, a lot of theoretical effort has gone into explaining the occurrence of unconventional superconductivity (SC) in strongly correlated electron systems (for a recent review see [1]). A basic model of interest here is the one-band Hubbard model which describes lattice fermions interacting with a strong on-site Coulomb repulsion. There is a general belief that in two dimensions (2D), this model qualitatively describes the normal state properties of high temperature superconductors (HTSC). Despite its simple form this model is difficult to analyze, and many of its properties remain to be understood.

The half filled Hubbard model is known to be an insulating antiferromagnet, and Quantum Monte Carlo results [1] and results from Hartree-Fock theory [2] indicate that antiferromagnetic (AF) correlations remain important up to quite high doping levels (at least for parameters adequate for HTSC). Moreover, short-range AF correlations in HTSC persist into the superconducting (SC) phase, as is seen e.g. in neutron-scattering experiments [3].

This provides strong motivation to study the consequences of antiferromagnetic correlations on superconductivity. Several different scenarios have been explored in the literature. For example: One much studied model is based on fermion pairing due to exchange of AF spin fluctuations [4]. Another is the spin bag mechanism which is based on the idea that local suppression of the AF gap leads to an effective attraction between certain quasiparticles, and thus to superconductivity [5]. Recently Dagotto and coworkers proposed and studied weak coupling models of holes in an antiferromagnet, using a numerically determined dispersion relation [6]. All these models lead to $d_{x^2-y^2}$ pairing, which indeed seems to be observed in experiments on HTSC [7]. To gain further insight it is useful both to try to carefully derive such effective models from the Hubbard model, and to calculate the physical properties and compare with experiments. Both these issues are addressed in this paper.

We study a lattice fermion model which gives a simple weak coupling description of superconductivity (SC) in the presence of antiferromagnetic (AF) correlations. In this model, the AF correlations are represented by an external, staggered magnetic field coupling to the fermion spin, and we include an attractive, instantaneous fermion-fermion interaction which can have on-site, nearest neighbor and next-nearest neighbor attractive couplings (the model is defined precisely in Section II A). The first purpose of the paper is to provide motivation for our effective model and develop an efficient formalism to carefully analyze this model. As will be discussed in more detail in Sections II B and II C, this model not only describes the effect of AF on SC in HTSC, but it actually is a general effective model for systems where AF correlations and SC coexist, e.g. also for certain heavy fermion systems [8] or materials where AF long range order coexists with SC [9]. To study this model, we use a flexible path integral formalism [10] which allows us to derive the mean field equations for our model in a simple way. The latter appear as generalization of BCS equations, but they turn out to be quite complicated and different from what might have naively been expected. In particular, our formulation can help to avoid difficulties associated with finding the relevant saddle points in the evaluation of the partition function [11]. Moreover, our formalism provides an efficient tool for deriving corrections to mean field theory (e.g. due to fluctuations; this will not be done in the present paper, though), and it is straightforward to adapt to other models. The second purpose of the paper is to calculate

some physical properties of this effective model in two dimensions and for parameters motivated by HTSC. In particular, we present a systematic analysis of the different possible SC channels. We find that the dominating channels are neither translation- nor spin rotation invariant, and a nearest neighbor attraction is most efficient in producing SC in presence of AF correlations. Moreover, the most stable channel usually has a $d_{x^2-y^2}$ -wave gap, $\Delta \propto \cos(k_1) - \cos(k_2)$. We will also give a simple, intuitive explanation of these results. We believe that this sheds some light on why $d_{x^2-y^2}$ -wave pairing was found in several different models for HTSC [4–6], as mentioned. Moreover, the gap equations in the full temperature range below T_c are derived and evaluated. Our formalism is a convenient starting point to evaluate physical properties of our model in the SC state, and these are quite different from the corresponding results for a standard BCS model. As an example, we evaluate the SC density of states and the resulting tunneling conductance as a function of temperature and find that it shows some of the features of experimental data of HTSC [12].

We will now describe one idea which we explore in this work, namely that AF correlations can drastically stabilize superconductivity [13,14]. Intuitively the reason for this is that AF correlations make the fermion bands much narrower. If the Fermi energy lies in such a band, the density of states at the Fermi surface (DOS) is increased. The SC critical temperature depends exponentially on the DOS and thus can increase by several orders of magnitude. Using parameters adequate for HTSC, we will see that a significant T_c only arises for unrealistically large couplings if there are no AF correlations. In presence of AF correlations, however, already modest couplings (as can arise by phonons, e.g.) can produce high T_c . This effect is quite dramatic. For example, for a standard BCS model with a tight binding band relation $\epsilon(\mathbf{k}) = -2t(\cos(k_1) + \cos(k_2))$ ($-\pi \leq k_i \leq \pi$) with $t = 0.5\text{eV}$ (which is a reasonable parameter for HTSC [1]), a coupling of $g_{BCS} = 0.05\text{eV}$ can lead only to a T_c of about 1 K or less. Assuming AF order with a magnitude of the order parameter of about 2.5eV (which is adequate for HTSC), we get $T_c \gtrsim 50$ K. We note that this DOS effect has also played an important role in other models motivated by HTSC [5,6], but the details of the scenarios suggested in these latter papers are different from ours. Moreover, even though this DOS effect is similar to the van Hove scenario for HTSC [15] in that a peak in the DOS is important for boosting T_c , it is different since the logarithmic singularity in the 2D DOS is not the essential point but rather the increase of the DOS by AF.

We finally note that our mean field analysis here only allows to determine the *magnitude* of the SC order parameter but *not* its *phase*. Thus nontrivial solutions of our mean field equations do not contradict the well-known fact that long-range order in the phase of the SC order does not exist in two dimensions.

The plan of this paper is as follows. In Section II we

give a detailed description of the model (II A) and then argue that it provides an effective description of the Hubbard model with an additional weak pairing interaction (II B). We also derive our model from the periodic Anderson model for heavy fermions [8] there (II C). Our analysis of the model starts in Section III, where we summarize the path integral formalism. The mean field equations are obtained in Section IV. We first (Sect. IV B) obtain the T_c -equations for all possible superconducting channels (singlet, and triplet, translational-invariant and staggered, s -, p - and d -wave) which are needed in our systematic stability analysis, and then (Sect. IV C) derive the gap Eqs. below T_c for the dominating channels. Section V contains our numerical results of our stability analysis, the temperature dependence of the SC gap, and the density of states and the tunneling conductance as a function of $T < T_c$. We end with conclusions in Section VI. Some technical details and calculation tricks are collected in two appendices.

II. THE MODEL

In this Section we present our model (A). We then give arguments that this model provides an effective description of SC in the doped Hubbard model (B) and the periodic Anderson model (C). It thus should be an effective model for HTSC and heavy fermion systems.

A. Model description

Our model Hamiltonian describes lattice fermions with field operators $a_{\uparrow,\downarrow}^{(+)}(\mathbf{x})$ in an external staggered magnetic field $\mathbf{B}(\mathbf{x})$ and an additional weak attractive BCS-like interaction,

$$H_{\text{eff}} = H_{\text{hop}} + \sum_{\mathbf{x}} \mathbf{S}(\mathbf{x}) \cdot \mathbf{B}(\mathbf{x}) e^{i\mathbf{Q} \cdot \mathbf{x}} + H_{\text{int}} \quad (2.1)$$

where $\mathbf{B} = (B_1, B_2, B_3)$ is the staggered magnetic field representing the AF order,

$$H_{\text{hop}} = - \sum_{\langle \mathbf{x}, \mathbf{y} \rangle, \sigma} t a_{\sigma}^{+}(\mathbf{x}) a_{\sigma}(\mathbf{y}) \quad (2.2)$$

is the usual hopping Hamiltonian (i.e. the sum is over all ordered pairs of nearest-neighboring sites $\langle \mathbf{x}, \mathbf{y} \rangle$ in \mathbb{Z}^d), $\mathbf{S} = a^{+}(\mathbf{x}) \boldsymbol{\sigma} a(\mathbf{x})$ is 2 times the electron spin operator ($\boldsymbol{\sigma}$ are the Pauli spin matrices), and

$$H_{\text{int}} = \frac{1}{2} \sum_{\mathbf{x}, \mathbf{y}} n(\mathbf{x}) V(\mathbf{x} - \mathbf{y}) n(\mathbf{y}), \quad n = \sum_{\sigma} a_{\sigma}^{+} a_{\sigma} \quad (2.3a)$$

is a (weak) attractive charge-charge interaction. We consider the model on a d -dimensional cubic lattice \mathbb{Z}^d (i.e. spatial vectors are $\mathbf{x} = (x_1, \dots, x_d)$ with x_i integers), and

$\mathbf{Q} = (\pi, \dots, \pi)$ is the usual AF vector. We use a pairing potential with the Fourier transform

$$V(\mathbf{k}) = -g_0 - g_{nn} \sum_i 2 \cos(k_i) - g_{nnn} \sum_{i \neq j} 2 \cos(k_i) \cos(k_j) \quad (2.3b)$$

where $\mathbf{k} = (k_1, \dots, k_d)$ with $-\pi \leq k_i \leq \pi$ and $g_i > 0$. The first, second and third terms here describe on-site, nearest neighbor (nn) and next-to-nearest neighbor (nnn) instantaneous interactions. We take the corresponding couplings g_i as input parameters of our model. A useful way to think about this potential is as coming from a Taylor expansion of some general potential $V(\mathbf{x} - \mathbf{y})$, where only the lowest order terms are kept since they are the only ones expected to be important for SC. Note that the normalization in Eq. (2.3b) is such that $V(\mathbf{x} - \mathbf{y})$ is $-g_0$, $-g_{nn}$ and $-g_{nnn}$ if \mathbf{x} and \mathbf{y} are equal, nn, and nnn, respectively. We do not fix dimension in our formal manipulations, but in our numerical calculations we take $d = 2$.

We will analyze the model setting $\mathbf{B}(\mathbf{x})$ independent of \mathbf{x} . Thus our results should be, in any case, of interest for materials where AF long range order coexisting with SC has been observed, see e.g. [9]. However, we expect that the results are also adequate for the case of varying staggered magnetic fields $\mathbf{B}(\mathbf{x})$ and thus for HTSC and heavy fermion systems. Arguments for this will be given below. In particular, it is important to note the following: even though the second term in Eq. (2.1) explicitly breaks spin rotation invariance, this model nevertheless describes also situations where this symmetry is unbroken: in such cases one can think of Eq. (2.1) as coming from a Born–Oppenheimer type approximation of a strong-coupling model which also describes dynamical AF correlations, and spin rotation invariance will be restored after averaging over certain $\mathbf{B}(\mathbf{x})$ -configurations. Especially, many of our results depend only on the magnitude $|\mathbf{B}(\mathbf{x})|$, and thus are, in a first approximation, equal to what one gets after averaging over the directions of $\mathbf{B}(\mathbf{x})$.

B. Effective description of the Hubbard model

Here we sketch an argument that our model gives an effective description of the doped Hubbard model extended by the attractive interaction H_{int} in Eq. (2.3a) (details are given elsewhere [11]). The idea is that the Coulomb repulsion between the electrons in mean field theory is replaced by an external staggered magnetic field. This is accomplished by a Hubbard–Stratonowitch transformation which allows the exact partition function of the Hubbard model to be rewritten in terms of non-selfinteracting fermions coupled to a dynamical boson field [16]

$$\phi_0(x) = r(x), \quad \phi(x) = \mathbf{B}(x) e^{i\mathbf{Q} \cdot \mathbf{x}} \quad (2.4)$$

where $s(x) = |\mathbf{B}(x)|$ and $\mathbf{e}(x) = \mathbf{B}(x)/|\mathbf{B}(x)|$ can be interpreted as magnitude and direction of the AF ordered fermion spins, and $r(x)$ represents a fermion charge [we write $x = (\tau_x, \mathbf{x})$ with τ_x the usual imaginary Matsubara time]. The stationary points in this exact path integral are the solutions of the Hartree–Fock equations. Quantum Monte Carlo results [17] indicate that these configurations are indeed dominant. Numerical results show that the Hartree–Fock solutions exhibit antiferromagnetic correlations, which are, however, spatially inhomogeneous: there are domain walls or magnetic vortices [i.e. $s(x)$ and $\mathbf{e}(x)$ depend on x]. This means that there may be many stationary points which have almost the same weight. The nontrivial assumption needed to justify our model is that all these solutions essentially describe AF bands, and that the chemical potential μ is in one of the AF bands, which, close to μ , have a DOS which can be well approximated by the simple AF bands coming from our model. An argument to justify this assumption is as follows. For thin domain walls, or localized vortices, $r(x) = r$ and $\mathbf{B}(x) = \mathbf{B}$ are constant in large regions of configuration space. Thus the states with energies in the AF bands correspond to wave functions which, for most x , coincide with one for constant $r(x) = r$ and $\mathbf{B}(x) = \mathbf{B}$ and thus are essentially the same as for the model we study (one can, for example, think of them as the scattering solutions in a domain wall background). The crucial assumption leading to our effective model is that the Fermi level is *in* an AF band. If this is the case, we expect that our model gives a good description of the states *close to the Fermi surface*. We note that there is direct support of this assumption from recent Monte Carlo calculations of the Hubbard model which show that for parameters adequate for HTSC, μ indeed intersects a peak in the DOS at a doping level $x \approx 0.15$ [18].

From this argument we see that the filling ρ used in our model is not equal to the corresponding filling in the Hubbard model: $\rho - 1$ is the doping of the AF band, which is smaller than the total doping if part of the charge carriers are bound in domain walls etc. The latter are not considered in our model since we expect that these charge carriers do not participate in SC.

As mentioned, we analyze the model setting $\mathbf{B}(\mathbf{x})$ independent of \mathbf{x} , but we expect our results are a good approximation also for the case of varying staggered magnetic fields $\mathbf{B}(\mathbf{x})$. One argument for this was already given: it is only important to approximate those states well that are close to the Fermi surface. A complementary argument for this is as follows: In case of a staggered magnetic field $B(x)$ which varies slowly or only in small fractions of space and time, the 2-point Green functions of our model can be approximated by

$$G(x, y) \approx G_N(x - y, y) + G_A(x - y, y) e^{i\mathbf{Q} \cdot \mathbf{y}} \quad (2.5)$$

where $G_{N,A}$ depends on the second argument y only via $\mathbf{e}(y) \cdot \boldsymbol{\sigma}$ and $s(y)$. These Green functions can be obtained

from the ones for $\mathbf{B}(y) = s\mathbf{e} = \text{const}$ by an expansion. In particular, thermodynamic properties only depend on $s(y)$ in this approximation. In case $s(y) \approx \text{const.}$, we thus expect that the thermodynamic properties of our model should not depend much on the AF correlation length (assuming the latter is large enough). In case also $s(y)$ changes but its changes only occur in small fractions of space and time, the thermodynamic properties are appropriate averages of the ‘local’ properties which can be deduced from the results in this paper.

C. Effective description of the periodic Anderson model

Here we present an argument that our model, with constant \mathbf{B} , can be obtained from the periodic Anderson model in a certain parameter regime. The physical picture is as follows: the periodic Anderson model is a 3D lattice fermion model with two kinds of spin- $\frac{1}{2}$ fermions: f -electrons with a strong Hubbard repulsion are coupled weakly to non-selfinteracting a -electrons [8]. For large on-site repulsion, the f -electrons can be regarded as half filled and antiferromagnetically ordered. The lower magnetic f -band is then far underneath the Fermi surface and the upper one far above. Thus the f -electrons are in a half-filled band and thus act as a commensurate [$\mathbf{e}(x) = \text{const.}$] AF background for the weakly coupled a -electrons, and our model provides an effective weak-coupling description of these a -electrons.

We now turn to a more detailed argument. We start from the following version periodic Anderson Hamiltonian

$$H = H_{\text{hop}} + H_f + V_{fa} + H_{\text{int}} \quad (2.6a)$$

where H_{hop} and H_{int} are as above, and

$$H_f = \sum_{\mathbf{x}} \left(-\epsilon_f n_f(\mathbf{x}) + U n_{f,\uparrow}(\mathbf{x}) n_{f,\downarrow}(\mathbf{x}) \right) \quad (2.6b)$$

describes another species of electrons denoted as f which are localized and have a strong on-site charge-charge repulsion $U \gg \epsilon_f \gg t$ ($n_{f,\sigma}(\mathbf{x}) = f_{\sigma}^{+}(\mathbf{x}) f_{\sigma}(\mathbf{x})$, and $n_f = n_{f,\uparrow} + n_{f,\downarrow}$). The interaction of the a and f electrons is local,

$$V_{fa} = \lambda \sum_{\mathbf{x}} \left(a_{\sigma}^{+}(\mathbf{x}) f_{\sigma}(\mathbf{x}) + f_{\sigma}^{+}(\mathbf{x}) a_{\sigma}(\mathbf{x}) \right), \quad (2.6c)$$

and H_{int} is as in Eq. (2.3a) i.e., we assume the BCS attraction among the a electrons only. $H_a + H_f + V_{fa}$ is the Anderson Hamiltonian: H_f is the usual strongly repulsive Hubbard Hamiltonian (with hopping constant $t_f \rightarrow 0$) which in the half-filled case (one f -electron per site) describes antiferromagnetically ordered electrons. The a -electrons are assumed in the conduction band weakly coupled to the f -electrons, and since $U \gg \epsilon_f \gg \lambda^2$

and $\epsilon_f \gg t$, one still expects the f electrons to form a half-filled antiferromagnet.

The simple physical picture leading to the effective Hamiltonian H_{eff} is that the coupling between the f and a electrons and the antiferromagnetic ordering of the former produces an effective staggered magnetic field that couples to the spin of the a electrons. The staggered magnetic field \mathbf{B} is determined by the interband coupling (see below). This effect is independent of the filling in the a band, because the antiferromagnetism comes from the f band, which is half-filled. This makes the situation simpler than in the non-half-filled repulsive Hubbard model, where commensurate order cannot be assumed.

In the remainder of this section, we derive H_{eff} from H by an argument patterned after Anderson’s derivation of the Heisenberg antiferromagnet from the half-filled Hubbard model.

We do a second-order perturbation expansion in λ to show that the coupling between the a and the f electrons produces the staggered field term of the effective Hamiltonian. For $\lambda = 0$, the ground state wave function factors into the product of that of the ground state for the a and the f . Since the f system is half-filled because U is large, the ground state wave function for the f electrons is

$$| \text{N\'eel} \rangle = \prod_{\mathbf{x}} f_{\sigma}^{+}(\mathbf{x}) | 0 \rangle, \quad \sigma(\mathbf{x}) = e^{i\mathbf{Q} \cdot \mathbf{x}} \quad (2.7)$$

where $| 0 \rangle$ denotes the empty state (and $\sigma(\mathbf{x})$ means \uparrow if $+1$ and \downarrow otherwise). The Hilbert space of the total system is the sum of the two orthogonal subspaces \mathcal{H}_a and \mathcal{H}_f . Correspondingly, the Hamiltonian has the matrix structure ($V_{fa} = \lambda V$ and $H_a = H_{\text{hop}} + H_{\text{int}}$)

$$H = \begin{pmatrix} H_a & V_{fa} \\ V_{fa} & H_f \end{pmatrix} = H_0 + \begin{pmatrix} 0 & \lambda V \\ \lambda V & 0 \end{pmatrix}. \quad (2.8)$$

The potential term appears off-diagonal because it couples the two subspaces. The resolvent is also a matrix, and the resolvent equation

$$\begin{aligned} \frac{1}{E - H} &= \frac{1}{E - H_0} + \frac{1}{E - H_0} V_{fa} \frac{1}{E - H} \\ &= \frac{1}{E - H_0} + \frac{1}{E - H_0} V_{fa} \frac{1}{E - H_0} \\ &+ \frac{1}{E - H_0} V_{fa} \frac{1}{E - H_0} V_{fa} \frac{1}{E - H} \end{aligned}$$

reads, denoting $R_a = (E - H_a)^{-1}$ and $R_f = (E - H_f)^{-1}$,

$$\begin{aligned} \frac{1}{E - H} &= \begin{pmatrix} R_a & 0 \\ 0 & R_f \end{pmatrix} + \lambda \begin{pmatrix} 0 & R_a V R_f \\ R_f V R_a & 0 \end{pmatrix} \\ &+ \lambda^2 \begin{pmatrix} R_a V R_f V & 0 \\ 0 & R_f V R_a V \end{pmatrix} \frac{1}{E - H}. \quad (2.9) \end{aligned}$$

We want to calculate the effective propagation of the a electrons to second order in λ . For this we need only the left upper element $R_{\text{eff}} = \left(\frac{1}{E - H} \right)_{aa}$. It is given by

$$R_{\text{eff}} = R_a + \lambda^2 R_a V R_f V R_{\text{eff}} \quad (2.10)$$

or in other words

$$R_{\text{eff}}^{-1} = E - H_a - \lambda^2 V R_f V \quad (2.11)$$

Up to this point, everything was exact. Now we approximate by keeping only terms up to order λ^2 . Moreover, since we want to see the influence of the interaction in the ground state only, we may calculate $V R_f V$ by its expectation with respect to f , taken in the state $|\text{N\'eel}\rangle$. This gives a staggered magnetic field term

$$\frac{1}{E + \epsilon_f + U} \sum_{\mathbf{x}} a^+(\mathbf{x}) \sigma_3 a(\mathbf{x}) e^{i\mathbf{Q}\cdot\mathbf{x}} \quad (2.12)$$

Finally, we want to define the effective Hamiltonian H_{eff} by $R_{\text{eff}}^{-1} = E - H_{\text{eff}}$. To do so, we note that the energy E is in the a band, so $|E| \leq 2t \ll \epsilon_f + U$, and thus we may replace $\frac{1}{E + \epsilon_f + U}$ by $\frac{1}{\epsilon_f + U}$. With this approximation, R_{eff}^{-1} depends only linearly on E , and, up to an uninteresting shift in the energy,

$$H_{\text{eff}} = H_a + \frac{\lambda^2}{\epsilon_f + U} \sum_{\mathbf{x}} a^+(\mathbf{x}) \sigma_3 a(\mathbf{x}) e^{i\mathbf{Q}\cdot\mathbf{x}} \quad (2.13)$$

is the effective Hamiltonian. Since H_{int} couples only the a electrons, it does not play a role in this argument. The coupling also produces a backreaction on the f electrons, but this influences the a electrons only in higher order in λ . This shows that a model of the type we study is induced, but the B field obtained by this argument is small.

III. FORMALISM

A. Functional integrals and mean field approximation

To study our effective model, we use the path integral formalism [19]. It is equivalent to the Hamiltonian framework and more convenient for calculating the grand canonical partition function $Z = \text{Tr } e^{-\beta(H - \mu N)}$. Thus configuration space is labeled by $x = (\tau_x, \mathbf{x})$ where $0 < \tau_x < \beta$ is the usual imaginary time and \mathbf{x} are vectors in the d -dimensional cubic lattice \mathbf{Z}^d (i.e. we set the lattice constant equal to 1). Most of our calculations are for arbitrary d , but we are mainly interested in $d = 2$ or 3. In intermediate steps of our derivation we will implicitly assume that space is a finite square (cube) with a finite number L^d of points, but we will eventually take the thermodynamic limit $L \rightarrow \infty$.

To define our model we introduce fields at every point x which are Grassmann variables $\psi_\sigma(x)$ and $\bar{\psi}_\sigma(x)$ carrying a spin index $\sigma = \{\uparrow, \downarrow\}$. We group the spacetime argument x and the spin index σ to a single coordinate

$X = (x, \sigma)$, and set $\psi(X) = \psi_\sigma(x)$ etc. We also use convenient short hand notations $\sum_x \equiv \int_0^\beta d\tau_x \sum_{\mathbf{x} \in \Lambda}$ and $\sum_X = \sum_{x, \sigma}$ etc. The partition function of the model can then be written as a fermion path integral

$$Z = \int \mathcal{D}\bar{\psi} \mathcal{D}\psi e^{-\mathcal{A}} \quad (3.1)$$

where $\int \mathcal{D}\bar{\psi} \mathcal{D}\psi = \prod_{x, \sigma} \int d\bar{\psi}_\sigma(x) \int d\psi_\sigma(x)$ are Grassmann integrals [19]. The action of the model is $\mathcal{A} = \sum_X \bar{\psi}(X) (\partial_\tau - \mu) \psi(X) + \int_0^\beta H(\bar{\psi}, \psi) d\tau = \mathcal{A}_2 + \mathcal{A}_4$, with a quadratic part defining the free Green function, $\mathcal{A}_2 = -\sum_{X, Y} \bar{\psi}(X) G_0^{-1}(X, Y) \psi(Y)$, and a quartic interaction term

$$\mathcal{A}_4 = \frac{1}{2} \sum_{X, Y} V(X, Y) \bar{\psi}(X) \bar{\psi}(Y) \psi(Y) \psi(X) \quad (3.2)$$

The free Green function G_0 is given by (we suppress the spin indices)

$$G_0^{-1}(x, y) = \delta(\tau_x - \tau_y) \left(\left[\delta_{\mathbf{x}, \mathbf{y}} \left(-\frac{\partial}{\partial \tau_x} + \mu \right) - \epsilon(\mathbf{x} - \mathbf{y}) \right] \sigma_0 - \delta_{\mathbf{x}, \mathbf{y}} \mathbf{B} \cdot \boldsymbol{\sigma} e^{i\mathbf{Q}\cdot\mathbf{x}} \right) \quad (3.3)$$

where $\epsilon(\mathbf{x} - \mathbf{y})$ is the Fourier transform of the tight-binding band relation

$$\epsilon(\mathbf{k}) = -2 \sum_{j=1}^d t_j \cos(k_j) \quad (3.4)$$

with t_j the usual hopping parameters, and σ_i for $i = 1, 2, 3$ are the Pauli spin matrices and σ_0 is the 2×2 unit matrix. The potential

$$V(X, Y) = \delta(\tau_x - \tau_y) V(\mathbf{x} - \mathbf{y}) = V(Y, X) \quad (3.5)$$

is independent of spin; the Fourier transform of $V(\mathbf{x} - \mathbf{y})$ is given in Eq. (2.3b).

To derive mean field equations for possible superconducting states we now introduce auxiliary bilocal pair fields and thus decouple the fermion interaction (see e.g. [10]),

$$e^{-\mathcal{A}_4} = \int \mathcal{D}\Delta^* \mathcal{D}\Delta \exp \sum_{X, Y} \left(\frac{|\Delta(X, Y)|^2}{2V(X, Y)} - \frac{1}{2} \overline{\Delta(X, Y)} \psi(Y) \psi(X) - \frac{1}{2} \bar{\psi}(X) \bar{\psi}(Y) \Delta(X, Y) \right) \quad (3.6)$$

where

$$\mathcal{D}\Delta^* \mathcal{D}\Delta = \prod_{\{X, Y\}} \frac{d\text{Re}\Delta(X, Y) d\text{Im}\Delta(X, Y)}{2\pi|V(X, Y)|} \quad (3.7)$$

is the measure for a complex boson path integral. The product runs only over those unordered pairs $\{X, Y\}$ for

which $V(X, Y) \neq 0$. We call the $\Delta(X, Y)$ Hubbard-Stratonovitch (HS) fields. Note that the integral over $\Delta(X, Y)$ is convergent because (and only if) the pairing potential is purely attractive, i.e. $V(X, Y) < 0$ whenever it is nonzero. Note also that due to the anticommutativity of the Grassmann variables only antisymmetric configurations,

$$\Delta(X, Y) = -\Delta(Y, X), \quad (3.8)$$

contribute to the path integral. Indeed, writing a general HS configuration as $\Delta = \Delta_+ + \Delta_-$ with $\Delta_{\pm}(X, Y) = [\Delta(X, Y) \pm \Delta(Y, X)]/2$, the Δ_+ decouple from the Fermion fields and thus only contribute a constant, irrelevant factor to the path integral [to see this, use $\psi(X)\psi(Y) = -\psi(Y)\psi(X)$, same for $\bar{\psi}$ and $V(X, Y) = V(Y, X)$, and rename the summation variables $X \leftrightarrow Y$]. Furthermore, since we are considering only an interaction which is instantaneous [see Eq. (3.5)], we also have that $\Delta(X, Y) = \Delta_{\sigma\sigma'}(\mathbf{x}, \mathbf{y}, \tau_x)\delta(\tau_x - \tau_y)$.

We now integrate out the fermions to rewrite the partition function Z as a boson (HS) path integral, as follows. We introduce Nambu fields

$$\Psi(X) = \begin{pmatrix} \psi(X) \\ \bar{\psi}(X) \end{pmatrix}, \quad \Psi^\dagger(X) = (\bar{\psi}(X), \psi(X)) \quad (3.9)$$

such that $\mathcal{A}_2 = -\frac{1}{2} \sum_{X, Y} \Psi^\dagger(X) \mathcal{G}_0^{-1}(X, Y) \Psi(Y)$ with

$$\mathcal{G}_0 = \begin{pmatrix} G_0 & 0 \\ 0 & \tilde{G}_0 \end{pmatrix}, \quad \tilde{G}_0(X, Y) = -G_0(Y, X) \quad (3.10)$$

the free Nambu Green function. Moreover,

$$\begin{aligned} \frac{1}{2} \sum_{X, Y} (\overline{\Delta(X, Y)} \psi(Y) \psi(X) + \bar{\psi}(X) \bar{\psi}(Y) \Delta(X, Y)) \\ = \frac{1}{2} \sum_{X, Y} \Psi^\dagger(X) \Sigma(X, Y) \Psi(Y) \end{aligned}$$

where

$$\Sigma = \begin{pmatrix} 0 & \Delta \\ \Delta^* & 0 \end{pmatrix}, \quad \Delta^*(X, Y) = \overline{\Delta(Y, X)}. \quad (3.11)$$

Thus

$$\begin{aligned} Z = \int \mathcal{D}\Psi \mathcal{D}\Delta^* \mathcal{D}\Delta \exp \frac{1}{2} \sum_{X, Y} \left(\frac{|\Delta(X, Y)|^2}{V(X, Y)} + \right. \\ \left. \Psi^\dagger(X) \mathcal{G}^{-1}(X, Y) \Psi(Y) \right) \end{aligned} \quad (3.12)$$

where $\int \mathcal{D}\bar{\psi} \mathcal{D}\psi \equiv \int \mathcal{D}\Psi$ and we define

$$\mathcal{G}^{-1} = \mathcal{G}_0^{-1} - \Sigma. \quad (3.13)$$

Integrating out the Nambu fields is easy now. We obtain

$$Z = \int \mathcal{D}\Delta^* \mathcal{D}\Delta e^{-\mathcal{F}(\Delta)} \quad (3.14)$$

with the effective HS action

$$\mathcal{F}(\Delta) = - \sum_{X, Y} \frac{|\Delta(X, Y)|^2}{2V(X, Y)} - \frac{1}{2} \text{Tr} \log(\mathcal{G}^{-1}) \quad (3.15)$$

where the second term come from the fermion path integral (logarithm of Pfaffian of \mathcal{G}^{-1} = half of logarithm of determinant of \mathcal{G}^{-1}). In the following we write

$$\mathcal{G} = \begin{pmatrix} G & F \\ F^* & \tilde{G} \end{pmatrix} \quad (3.16)$$

which is equal to the Green function for non-self-interacting fermions in an external field Δ . In this representation, the exact fermion two-point function is given by

$$\langle \Psi(X) \Psi(Y)^\dagger \rangle = -\frac{1}{Z} \int \mathcal{D}\Delta^* \mathcal{D}\Delta e^{-\mathcal{F}(\Delta)} \mathcal{G}. \quad (3.17)$$

The antisymmetry of the fermions, $\psi(X)\psi(Y) = -\psi(Y)\psi(X)$ implies $F(X, Y) = -F(Y, X)$.

Hartree-Fock (HF) theory amounts to evaluating the HS path integral in Eq. (3.14) using the saddle point method. We obtain $Z \approx \exp[-\mathcal{F}(\Delta_{HF})]$ where Δ_{HF} is the solution of the saddle point equation $\delta\mathcal{F}(\Delta)/\delta\Delta(X, Y) = 0$ which corresponds to the *minimum* of \mathcal{F} . More explicitly the (complex conjugate of the) latter equation is

$$\Delta(X, Y) = V(X, Y)F(X, Y) \quad (3.18)$$

which together with Eq. (3.13) forms a selfconsistent system of equations and provides the BCS description for our model. Note that in the saddle-point approximation, $-\langle \Psi(X) \Psi(Y)^\dagger \rangle = \mathcal{G}$, so Eq. (3.13) can now be interpreted as the Dyson equation for our electron Green function \mathcal{G} where mean field theory gives the approximation (3.18) for the electron self-energy Σ .

We now recall an important point: in mean field theory, the Pauli principle has to be imposed as a separate condition: the exact gap must be antisymmetric, $\Delta(X, Y) = -\Delta(Y, X)$ because V is symmetric and F is antisymmetric, as discussed above. However, (3.18) can have solutions Δ that violate this antisymmetry, and which are therefore unphysical. Therefore we *discard all solutions of our mean field equations which do not obey the condition (3.8)*. In our formalism, antisymmetry of Δ is already built in since we restricted the exact HS path integral to configurations obeying this condition [see (3.8)].

The general analysis of the mean field equations is still too difficult since for general X, Y dependent HS field configurations $\Delta(X, Y)$, the evaluation of the Nambu Green function (3.16) is impossible in general. To proceed we therefore make the usual assumption and only consider HS configurations that have at least a remnant of translation invariance. Since for our model the free Green function contains a staggered contribution i.e. is

not invariant under translations by *one* but only *two* sites, the simplest consistent ansatz for our HF equations are HS configurations Δ invariant by translations by two sites. We refer to HF theory together with such an ansatz for Δ as *mean field theory*.

IV. STAGGERED SUPERCONDUCTIVITY

A. Staggered states

We now specialize to time independent states where the superconducting order parameter has a uniform part and a staggered part, i.e. [20]

$$\Delta(\mathbf{x}, \mathbf{y}) = \Delta_N(\mathbf{x} - \mathbf{y}) + \Delta_A(\mathbf{x} - \mathbf{y})e^{i\mathbf{Q}\cdot\mathbf{y}}, \quad (4.1)$$

with $\mathbf{Q} = (\pi, \dots, \pi)$ the antiferromagnetic vector (here and below we use spin matrix notation whenever possible). This obviously implies that \mathcal{G} is also a sum of a uniform and staggered contribution, and we can solve the Dyson equation (3.13) by Fourier transform.

Our convention for Fourier transformation is

$$f(x) = \sum_k e^{-ikx} f(k), \quad kx = \omega_n \tau_x - \mathbf{x} \cdot \mathbf{k}$$

where $k = (\omega_n, \mathbf{k})$ with $\omega_n = \frac{(2n+1)\pi}{\beta}$ ($n \in \mathbb{Z}$) the Matsubara frequencies and $\mathbf{k} = (k_1, \dots, k_d)$ a momentum vector in the first Brillouin zone $[-\pi, \pi]^d$ of the lattice, i.e.

$$\sum_k \equiv \frac{1}{\beta} \sum_{\omega_n} \int d\mathbf{k}, \quad \int d\mathbf{k} \equiv \int_{[-\pi, \pi]^d} \frac{d^d \mathbf{k}}{(2\pi)^d}.$$

Then $f(k) = \sum_x e^{ikx} f(x)$.

With that the self-energy equation (3.18) becomes

$$\Delta_{N,A}(k) = \sum_q V(k - q) F_{N,A}(q). \quad (4.2)$$

B. T_c -equations

For simplicity we first consider the region close to the critical temperature T_c where the Dyson equation (3.13) can be linearized in the non-gauge invariant Green functions F and self-energy Δ . Writing (3.13) as $\mathcal{G} = \mathcal{G}_0 + \mathcal{G}_0 * \Sigma * \mathcal{G}_0 + \dots$ we obtain the linearized equation $F = G_0 * \Delta * \tilde{G}_0$ i.e.

$$F(x, y) = \sum_{z_1, z_2} G_0(x, z_1) \Delta(z_1, z_2) \tilde{G}_0(z_2, y) \quad (4.3)$$

where $\tilde{G}_0(x, y) \equiv -G_0(y, x)^T$ and T means matrix transposition. With the ansatz (4.1) and Fourier transform

this becomes (the k dependence is suppressed, $F_N \equiv F_N(k)$ etc., in the following),

$$\begin{aligned} F_{N,A} &= G_{0N} \Delta_N \tilde{G}_{0N,A} + G_{0A} \Delta_N^Q \tilde{G}_{0A,N}^Q \\ &\quad + G_{0A} \Delta_A^Q \tilde{G}_{0N,A} + G_{0N} \Delta_A \tilde{G}_{0A,N}^Q \end{aligned} \quad (4.4)$$

where $\Delta_N^Q(k) = \Delta_N(k - Q)$ etc, and spin matrix multiplication is understood. Combined with Eq.(4.2), this gives the T_c equations for our model.

The translation-invariant and staggered parts of the free Green function, $G_{0N,A}$, are (see Appendix A)

$$G_{0N}(k) = g(k) \sigma_0, \quad G_{0A}(k) = a(k) \sigma_3 \quad (4.5a)$$

where

$$\begin{aligned} g(k) &= \frac{i\omega_n + \mu + \epsilon(\mathbf{k})}{(i\omega_n - E_+)(i\omega_n - E_-)} \\ a(k) &= \frac{s}{(i\omega_n - E_+)(i\omega_n - E_-)} \end{aligned} \quad (4.5b)$$

[we used $\epsilon(\mathbf{k} + \mathbf{Q}) = -\epsilon(\mathbf{k})$] and

$$E_{\pm}(\mathbf{k}) = -\mu \pm \sqrt{\epsilon(\mathbf{k})^2 + s^2} \quad (4.6)$$

are the antiferromagnetic bands. We also set $\mathbf{B} \cdot \boldsymbol{\sigma} = s\sigma_3$ without loss of generality.

To deal with the remaining dependence on the relative coordinate, $\mathbf{x} - \mathbf{y}$, we decompose the order parameter $\Delta_{N,A}$ in components that transform according to the irreducible representations of the lattice point group:

$$\Delta(\mathbf{x} - \mathbf{y}) = \sum_J \Delta_J \eta_J(\mathbf{x} - \mathbf{y}). \quad (4.7)$$

For a two dimensional square lattice the functions η_J we need are listed in Table I. They are orthonormal, $\int d\mathbf{k} \eta_J(\mathbf{k}) \eta_{J'}(\mathbf{k}) = \delta_{JJ'}$. These functions determine the shape of the gap, i.e., if it is *s*-wave or *d*-wave etc. The potential (2.3b) has the expansion

$$V(\mathbf{k} - \mathbf{q}) = - \sum_J g_J \eta_J(\mathbf{k}) \eta_J(\mathbf{q}). \quad (4.8)$$

where

$$\begin{aligned} g_1 &= g_2 = g_3 = g_4 = g_{nn} \\ g_5 &= g_6 = g_7 = g_8 = g_{nnnn}. \end{aligned} \quad (4.9)$$

Note that the interaction V , which is a diagonal matrix in the x -basis (i.e., it acts by ordinary multiplication) in Eq. (3.18), is still diagonal in the new basis. This is because the coupling constants g_0 , g_{nn} and g_{nnnn} are the same for all on-site, for all nearest neighbor and for all next nearest neighbor interactions, respectively, i.e., the interaction is proportional to identity within each of these subspaces, and because the unitary transformation implied by Eq. (4.7) does not mix these subspaces.

TABLE I. Symmetries of the order parameter.

Symmetry	On-site (0)	Nearest neighbor (nn)	Next nearest neighbor (nnn)
<i>s</i> -wave	$\eta_0(\mathbf{k}) = 1$	$\eta_1(\mathbf{k}) = \cos(k_1) + \cos(k_2)$	$\eta_5(\mathbf{k}) = \cos(k_1 + k_2) + \cos(k_1 - k_2)$
<i>p</i> -wave		$\eta_{2,3}(\mathbf{k}) = \sin(k_1) \pm \sin(k_2)$	$\eta_{6,7}(\mathbf{k}) = \sin(k_1 + k_2) \pm \sin(k_1 - k_2)$
<i>d</i> -wave		$\eta_4(\mathbf{k}) = \cos(k_1) - \cos(k_2)$	$\eta_8(\mathbf{k}) = \cos(k_1 + k_2) - \cos(k_1 - k_2)$

Then we get coupled (linear algebraic) equations for the 2×2 matrices $(\Delta_{N,A})_J$. For simplicity we further neglect the ‘mixing of the different gap shapes’ i.e. restrict to configurations $\Delta_{N,A}(k) = (\Delta_{N,A})_J \eta_J(\mathbf{k})$ (no summation over J). This is appropriate whenever one of the shape functions η_J is dominating over all others. Our numerical results below confirm that this is the case for finite s which is what we are mainly interested in. We note that it would be straightforward (though much more work) to extend the following analysis to also allow for a mixing of different shapes, but this would be required only in case one would find two SC channels with different gap shapes and gaps of the same order of magnitude at the same temperature.

We write

$$\begin{aligned} \Delta_N(k) &= \begin{pmatrix} \Delta_{1,J} & \Delta_{2,J} \\ \Delta_{3,J} & \Delta_{4,J} \end{pmatrix} \eta_J(\mathbf{k}) \\ \Delta_A(k) &= \begin{pmatrix} \Theta_{1,J} & \Theta_{2,J} \\ \Theta_{3,J} & \Theta_{4,J} \end{pmatrix} \eta_J(\mathbf{k}) \end{aligned} \quad (4.10)$$

so that the $\Delta_{i,J}$ and $\Theta_{i,J}$ are the c-number order-parameters for the superconducting state. The final equations will give a critical temperature T_c for each of the possible channels separately, and the biggest of those determines the dominating channel and the T_c of the system.

In the following we suppress indices (J, i) and write

$$\eta \equiv \eta_J, \quad g_J \equiv g_{BCS}$$

etc.; it is understood that one has to calculate the critical temperatures for all interesting channels and take the maximum one. This determines the dominant SC channel: the ‘shape’ $\eta(\mathbf{k})$, the spin structure, and the ratio of translation invariant and staggered parts Δ and Θ of the gap.

Every shape function η can be characterized by two sign factors $p = +, -$ and $\xi = +, -$ defined by

$$\eta(\mathbf{k} - \mathbf{Q}) = p \eta(\mathbf{k}), \quad \eta(-\mathbf{k}) = \xi \eta(\mathbf{k}); \quad (4.11)$$

these determine which spin structures of the gap are compatible with the Pauli principle Eq. (3.8). Since in position space, the spatial dependence of $\Delta_{N,A}(\mathbf{x} - \mathbf{y})$ is given by the Fourier transform $\eta(\mathbf{x} - \mathbf{y}) = p \eta(\mathbf{x} - \mathbf{y}) e^{i\mathbf{Q} \cdot (\mathbf{x} - \mathbf{y})} = \xi \eta(\mathbf{y} - \mathbf{x})$ of $\eta(\mathbf{k})$, (3.8) implies the following conditions

$$\Delta_{1,4} = -\xi \Delta_{1,4}, \quad \Theta_{1,4} = -\xi p \Theta_{1,4} \quad (4.12a)$$

and

$$\Delta_2 = -\xi \Delta_3, \quad \Theta_2 = -\xi p \Theta_3. \quad (4.12b)$$

These conditions exclude many of the possible solutions of the mean field equations, e.g. all those where $\Delta_1 \neq 0$ with $\xi \neq -1$ and $\Theta_1 \neq 0$ with $\xi p \neq -1$ etc.

We now derive the T_c -equations for our model. As the potential is frequency independent we can do the Matsubara sums analytically. After a straightforward calculation (see Appendix B) we obtain

$$\begin{aligned} \Delta_{1,4} &= g_{BCS} K_p(\beta) \Delta_{1,4} \pm g_{BCS} L_p(\beta) \Theta_{1,4} \\ \Theta_{1,4} &= g_{BCS} \tilde{K}_p(\beta) \Theta_{1,4} \pm g_{BCS} L_p(\beta) \Delta_{1,4} \end{aligned} \quad (4.13a)$$

and

$$\begin{aligned} \Delta_{2,3} &= g_{BCS} K_{-p}(\beta) \Delta_{2,3} \mp g_{BCS} L_{-p}(\beta) \Theta_{2,3} \\ \Theta_{2,3} &= g_{BCS} \tilde{K}_{-p}(\beta) \Theta_{2,3} \mp g_{BCS} L_{-p}(\beta) \Delta_{2,3} \end{aligned} \quad (4.13b)$$

where $p = \pm$ is determined by $\eta(\mathbf{k})$ as above, and the functions $K_{\pm}(\beta)$ etc. are given in Appendix B. In fact $L_- = 0$, therefore half of the combinations will lead to uncoupled equations for the staggered and translation invariant gaps.

In the following we list the possible channels $\Delta(\mathbf{x}, \mathbf{y})$. We use the following notation for the spin matrix structure

$$|\uparrow\uparrow\rangle = \begin{pmatrix} 1 & 0 \\ 0 & 0 \end{pmatrix}, \quad |\uparrow\downarrow\rangle = \begin{pmatrix} 0 & 1 \\ 0 & 0 \end{pmatrix}, \quad \text{etc.} \quad (4.14)$$

and η_J is short for $\eta_J(\mathbf{x} - \mathbf{y}) \equiv \int d\mathbf{k} e^{i\mathbf{k} \cdot (\mathbf{x} - \mathbf{y})} \eta(\mathbf{k})$ i.e. the Fourier transformed functions defined in Table I. We use obvious symbols Δ_s^0 etc. as abbreviations for the channels.

For on-site: $g_{BCS} = g_0$, $p = +1$,

$$\begin{aligned} \Delta_s^0 &: \Delta(|\uparrow\downarrow\rangle - |\downarrow\uparrow\rangle) \eta_0 \\ \Theta_s^0 &: \Theta e^{i\mathbf{Q} \cdot \mathbf{y}} (|\uparrow\downarrow\rangle - |\downarrow\uparrow\rangle) \eta_0 \end{aligned} \quad (4.15a)$$

For nearest neighbor: $g_{BCS} = g_{nn}$, $p = -1$,

$$\begin{aligned} \Theta_s^{nn} &: \Theta e^{i\mathbf{Q} \cdot \mathbf{y}} \{|\uparrow\uparrow\rangle \text{ or } |\downarrow\downarrow\rangle\} \eta_1 \\ \Delta_p^{nn} &: \Delta \{|\uparrow\uparrow\rangle \text{ or } |\downarrow\downarrow\rangle\} \eta_{2,3} \\ \Theta_d^{nn} &: \Theta e^{i\mathbf{Q} \cdot \mathbf{y}} \{|\uparrow\uparrow\rangle \text{ or } |\downarrow\downarrow\rangle\} \eta_4 \\ (\Delta &\& \Theta)_s^{nn} : \left(\Delta(|\uparrow\downarrow\rangle - |\downarrow\uparrow\rangle) + \Theta e^{i\mathbf{Q} \cdot \mathbf{y}} (|\uparrow\downarrow\rangle + |\downarrow\uparrow\rangle) \right) \eta_1 \\ (\Delta &\& \Theta)_p^{nn} : \left(\Delta(|\uparrow\downarrow\rangle + |\downarrow\uparrow\rangle) + \Theta e^{i\mathbf{Q} \cdot \mathbf{y}} (|\uparrow\downarrow\rangle - |\downarrow\uparrow\rangle) \right) \eta_{2,3} \\ (\Delta &\& \Theta)_d^{nn} : \left(\Delta(|\uparrow\downarrow\rangle - |\downarrow\uparrow\rangle) + \Theta e^{i\mathbf{Q} \cdot \mathbf{y}} (|\uparrow\downarrow\rangle + |\downarrow\uparrow\rangle) \right) \eta_4 \end{aligned} \quad (4.15b)$$

(the two p -channels are always degenerate)

For next-to-nearest neighbor: $g_{BCS} = g_{nnn}$, $p = 1$,

$$\begin{aligned} \Delta_s^{nnn} &: \Delta (|\uparrow\downarrow\rangle - |\downarrow\uparrow\rangle) \eta_5 \\ \Delta_p^{nnn} &: \Delta (|\uparrow\downarrow\rangle + |\downarrow\uparrow\rangle) \eta_{6,7} \\ \Delta_d^{nnn} &: \Delta (|\uparrow\downarrow\rangle - |\downarrow\uparrow\rangle) \eta_8 \\ \Theta_s^{nnn} &: \Theta e^{i\mathbf{Q}\cdot\mathbf{y}} (|\uparrow\downarrow\rangle - |\downarrow\uparrow\rangle) \eta_5 \\ \Theta_p^{nnn} &: \Theta e^{i\mathbf{Q}\cdot\mathbf{y}} (|\uparrow\downarrow\rangle + |\downarrow\uparrow\rangle) \eta_{6,7} \\ \Theta_d^{nnn} &: \Theta e^{i\mathbf{Q}\cdot\mathbf{y}} (|\uparrow\downarrow\rangle - |\downarrow\uparrow\rangle) \eta_8 \\ (\Delta\&\Theta)_p^{nnn} &: \begin{cases} (\Delta + \Theta e^{i\mathbf{Q}\cdot\mathbf{y}}) |\uparrow\uparrow\rangle \eta_6 \\ (\Delta - \Theta e^{i\mathbf{Q}\cdot\mathbf{y}}) |\downarrow\downarrow\rangle \eta_7 \end{cases} \end{aligned} \quad (4.15c)$$

Note that some of the gaps are a mixture of spin singlet and triplet. This comes as no surprise since spin rotation symmetry is broken in our model.

We finally note that one can easily derive BCS-like T_c -equations from (4.13). It is easy to see that for large β (small temperatures) and finite s , a nontrivial filling $\rho \neq 1$ is only possible for $s \approx w \approx |\mu|$, thus

$$|K_+| \approx |\tilde{K}_+| \approx |L_+| \approx M \log(\Omega\beta), \quad (4.16)$$

and K_- , \tilde{K}_- are much smaller in comparison (explicit formulas for these constants are derived in Appendix B). The constant

$$M = \int d\mathbf{k} \frac{1}{2} (\delta(E_+) + \delta(E_-)) \eta(\mathbf{k})^2 \quad (4.17)$$

has the natural interpretation as DOS $N_s(\mu)$ times the Fermi surface average of $\eta(\mathbf{k})^2$ (shape of the SC gap squared), and Ω can be regarded as an effective energy cutoff of the interaction. Thus we get a BCS like equation

$$T_c = \Omega e^{-1/g_{BCS}\Lambda} \quad (4.18)$$

with $\Lambda = 2M$, which can be trusted as long as T_c is small. This already allows us to make predictions about the most stable channels for large s -values: the channels where Δ and Θ are decoupled should have a negligible T_c (due to the smallness of K_- and \tilde{K}_-) and thus should be irrelevant as compared to the mixed channels $(\Delta\&\Theta)$. Moreover, for the latter we should always find $\Theta \approx \pm\Delta$, at least for sufficiently large s . Thus in case of dominating nnn attraction one should expect the SC channel $(\Delta\&\Theta)_p^{nnn}$. In case of dominating nn attraction, also the shape of the gap matters, and one has to check which one leads to the biggest M i.e. the largest Fermi surface average of $\eta(\mathbf{k})^2$. For larger s -values, the Fermi surface is similar to the one of the half-filled hopping band (since the Fermi surface is given by $E_{\pm} = 0$ i.e. $\epsilon(\mathbf{k}) = \pm\sqrt{\mu^2 - s^2}$ which is ≈ 0 for larger s -values at finite doping), and η_4 leads to the biggest M (it is easy to see why η_1 cannot lead to a significant M : it is proportional to ϵ and thus ≈ 0 at the Fermi surface). Thus

for dominating nn attraction, one should expect the SC channel $(\Delta\&\Theta)_d^{nn}$.

We confirm this result in a systematic stability analysis of all channels in the next section. The $\Delta\&\Theta$ -structure of the dominating SC channel has a simple physical explanation: The density of electrons should follow the staggered magnetic field $\mathbf{B}e^{i\mathbf{Q}\cdot\mathbf{x}}$: denoting as \uparrow the spin directions in the direction of \mathbf{B} and \downarrow opposite to it, the density difference $\rho_{\uparrow}(\mathbf{x}) - \rho_{\downarrow}(\mathbf{x})$ of spin- \uparrow and spin- \downarrow fermions on the site \mathbf{x} should be proportional to $|\mathbf{B}|e^{i\mathbf{Q}\cdot\mathbf{x}}$. Thus one should expect that stable Cooper pairs can only arise from electrons with their spins in direction of $\mathbf{B}e^{i\mathbf{Q}\cdot\mathbf{x}}$ (otherwise the density of the participating electrons is very small). If both electrons are on the same site (on-site attraction), this is never possible and no significant SC is expected. In case the paired electrons are on adjacent sites (nn attraction), the preferred spin configuration is expected to be $|\uparrow\downarrow\rangle$ or $|\downarrow\uparrow\rangle$ (following the AF order), and there should be nearly no mixing of these two. Finally in the nnn case, the most stable Cooper pairs should be those with $|\uparrow\uparrow\rangle$ or $|\downarrow\downarrow\rangle$ (following the AF order).

C. Mean field theory below T_c

The mean field theory below T_c is obtained by minimizing the action, Eq. (3.15), for field configurations of the form given in Eq. (4.1). Introducing also the transformation (4.7) we can write the action as

$$\mathcal{F} = \beta L^d \sum_{J,\sigma,\sigma'} \frac{|\Delta_{J\sigma\sigma'}|^2 + |\Theta_{J\sigma\sigma'}|^2}{2g_J} - \frac{1}{2} \text{Tr} \log(\mathcal{G}^{-1}). \quad (4.19)$$

The second term in the action can be expressed as $\text{Tr} \log(\mathcal{G}^{-1}) = \frac{1}{2} \beta L^d \sum_k \log \det \mathcal{R}(k)$, where \mathcal{R} is the 8×8 -matrix given by

$$\mathcal{R} = \begin{pmatrix} R & -\Delta \\ -\Delta^* & \tilde{R} \end{pmatrix} \quad (4.20)$$

where $\tilde{R}(k) = -R^T(-k)$ with

$$R = \begin{pmatrix} R_N & R_A \\ R_A^Q & R_N^Q \end{pmatrix}, \quad \Delta = \begin{pmatrix} \Delta_N & \Delta_A \\ \Delta_A^Q & \Delta_N^Q \end{pmatrix} \quad (4.21)$$

and

$$R_N = [i\omega_n - (\epsilon(\mathbf{k}) - \mu)]\sigma_0, \quad R_A = -s\sigma_3. \quad (4.22)$$

As in the previous section we assume that only one channel will contribute, i.e., we put all g_J but one equal to zero. Then, with Eqs. (4.10), (4.12) and $\epsilon(\mathbf{k}) = \epsilon(-\mathbf{k}) = -\epsilon(\mathbf{k} - \mathbf{Q})$, the determinant can be evaluated by finding the eigenvalues E_c of \mathcal{R} :

$$\frac{1}{2} \log \det \mathcal{R}(k) = \sum_{c=1}^4 \log(i\omega - E_c(k)) \quad (4.23)$$

(since every eigenvalue is 2-fold degenerate). These eigenvalues describe the electron bands. For the dominant channels Δ & Θ in Eq. (4.15), these electron bands E_c are given by

$$E_{1,2} = \pm E_+ \quad E_{3,4} = \pm E_- \quad (4.24a)$$

with

$$\begin{aligned} E_{\pm} &= \sqrt{\epsilon^2 + \mu^2 + s^2 + |\Delta_N|^2 + |\Delta_A|^2 \pm 2W} \\ W &= \sqrt{\epsilon^2 |\Delta_A|^2 + \epsilon^2 \mu^2 + [\mu s + |\Delta_N| |\Delta_A| \cos(\phi)]^2} \\ \epsilon &= \epsilon(\mathbf{k}), \quad \Delta_N = \Delta \eta(\mathbf{k}), \quad \Delta_A = \Theta \eta(\mathbf{k}) \end{aligned} \quad (4.24b)$$

where ϕ is the relative phase of Δ and Θ ,

$$\Delta = |\Delta| e^{i(\alpha+\phi)}, \quad \Theta = |\Theta| e^{i\alpha} \quad (4.24c)$$

and the bands are independent of α . [We do not write down the formulas for the channels Δ and Θ in eq. (4.15) since they are irrelevant, as discussed.]

Performing the Matsubara sum we obtain

$$\mathcal{F} = \beta L^d f_0(\Delta, \Theta) \quad (4.25)$$

with

$$f_0 = \sum_{\sigma, \sigma'} \frac{|\Delta_{\sigma\sigma'}|^2 + |\Theta_{\sigma\sigma'}|^2}{2g_J} - \frac{1}{2} \sum_{c=1}^4 \int d\mathbf{k} \ln_{\beta}(E_c) \quad (4.26)$$

where we define

$$\frac{1}{\beta} \sum_n \log(i\omega_n - E) = \frac{1}{\beta} \log(1 + e^{-\beta E}) \equiv \ln_{\beta}(E) \quad (4.27)$$

We note that in this latter equation the sum is regularized: it is obtained by integrating $\frac{1}{\beta} \sum_n \frac{e^{i\omega_n 0^+}}{i\omega_n - E} = \frac{1}{1 + e^{\beta E}}$ and dropping an irrelevant infinite constant.

The mean field solution is now obtained by minimizing the action,

$$\Omega(\mu) = \min_{\Delta, \Theta} f_0(\Delta, \Theta) \quad (4.28a)$$

where we have to take the *absolute* minimum. Moreover, the chemical potential is fixed by filling,

$$\rho = -\frac{\partial \Omega}{\partial \mu}. \quad (4.28b)$$

The standard mean field equations are $\partial \mathcal{F} / \partial \Delta = \partial \mathcal{F} / \partial \Theta = 0$ and have, in general, several solutions which are not the absolute minimum and therefore have to be discarded. In the formulation eq. (4.28), the correct solution is selected automatically.

Clearly the minima will be invariant under global shifts of the phase α . Thus we end up with a simple minimization problem in the three parameters $|\Delta|, |\Theta|$ and ϕ . We find that the relative phase ϕ minimizes the action when W is minimized, i.e. $\cos \phi = -\text{sign}(\mu)$.

With the mean field solution at hand we can now proceed to calculate physical quantities. The Green function is given by the matrix inverse of $\mathcal{R}(k)$. As an important example, we recall that the superconducting one-particle density of states is obtained as

$$N(\omega) = -\frac{1}{\pi} \text{Im} \sum_{\sigma} \int d\mathbf{k} (G_N)_{\sigma\sigma}(\mathbf{k}, i\omega_n \rightarrow \omega + i0^+). \quad (4.29)$$

Due to the complexity of the bands, (4.24), this expression is much more complicated than the standard BCS result. The differential current-voltage dependence of the tunneling current between a superconductor and a normal metal is related to this by

$$\frac{dI}{dV} \propto \int N(\omega) \left(-\frac{\partial f_{\beta}(\omega - eV)}{\partial \omega} \right) d\omega, \quad (4.30)$$

where $f_{\beta}(E) = \frac{1}{e^{\beta E} + 1}$ is the usual Fermi-Dirac distribution, and e is the electron charge.

V. NUMERICAL RESULTS

In this section we describe the results of a numerical evaluation of the mean field equations in the previous section. The numeric evaluation was done by performing the Brillouin zone integrals using a standard integration routine. Since the integrands are typically strongly peaked, care was taken to ensure sufficiently small discretization errors by using an adaptive stepsize method. Moreover, we solved mean field equations by minimizing the function f_0 eq. (4.26) using standard numeric routines.

As discussed, we neglect possible mixing of gaps assuming that the dominating gap transforms under an irreducible representation of the symmetry group of the lattice (note that this is an approximation here since, in general, the energy dependence of the gap cannot be neglected as in ordinary BCS theory). We use the following parameters

$$t = 0.5 \text{ eV}, \quad g_{BCS} = 0.05 \text{ eV}, \quad 0 \leq s \leq 4 \text{ eV} \quad (5.1)$$

motivated by high temperature superconductors [1] (note that for the half filled Hubbard model, mean field theory predicts antiferromagnetic order with $s \approx U/2$).

The results in Figs. 1–3 were obtained by evaluating the T_c equations (4.13). To compare the stability of different gaps, we found it convenient to determine the required BCS coupling g_{BCS} to achieve a given critical temperature T_c . In Fig. 1, the required g_{BCS} is plotted as a function of the magnitude s of the AF order for all possible channels. We chose $\rho = 0.9$ and $T_c = 50 \text{ K}$ as representative examples. One can clearly see that the mixed channels Δ & Θ are the only ones which are enhanced by the antiferromagnetism and always dominate over the others. It is also always the same channels which

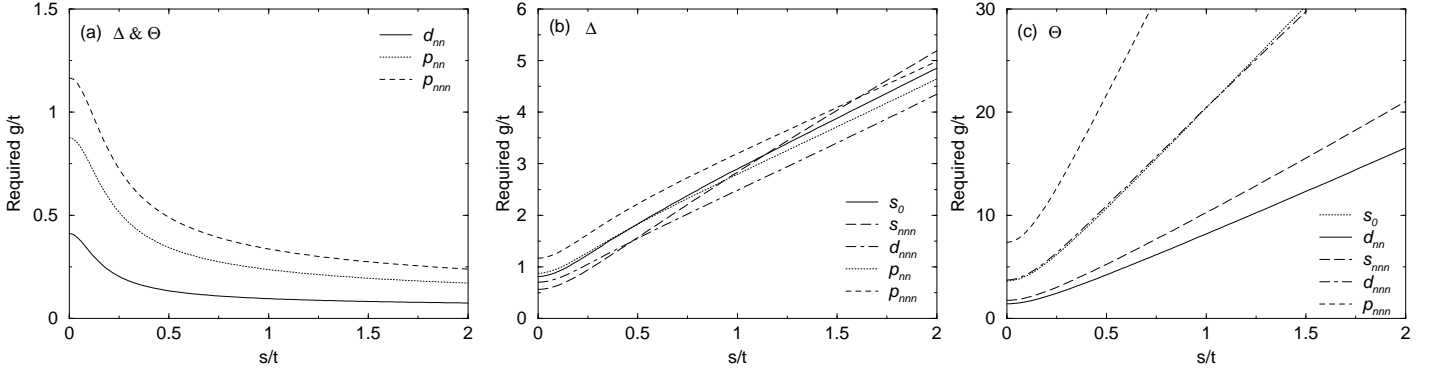


FIG. 1. Comparison of stability of different SC channels in 2D model: required BCS coupling g_{BCS} to achieve a given superconducting critical temperature $T_c = 100\text{K}(t/1\text{eV})$, as a function of the magnitude of the antiferromagnetic order s at fixed filling ρ for different shapes of the gap, which are listed in Table I. (For a hopping parameter $t = 0.5\text{ eV}$ adequate for HTSC this corresponds to $T_c = 50\text{ K}$). The filling $\rho = 0.9$ considered here is representative. (a): $\Delta\&\Theta$ -channel i.e. mixture of staggered and translation invariant gaps which we find to dominate throughout. (b): Δ -channel i.e. pure translation invariant gap. (c): Θ -channel, i.e. pure staggered gap. Note the different scales of the g_{BCS} -axes in the different plots. There is also a s_{nn} in both the mixed and purely staggered channel which requires an even higher coupling.

dominate: $(\Delta\&\Theta)_d^{nn}$ in case of a nearest neighbor attraction, and $(\Delta\&\Theta)_p^{nnn}$ in the next nearest neighbor case [cf. Eqs. (4.15)]. The latter one requires a much larger coupling g_{BCS} than the former, though. These results do not change qualitatively as the doping is changed over a wide parameter range. As s goes to zero the staggered part of the mixed channels decrease in comparison to the translation invariant part, so that they completely decouple at $s = 0$. This, however, happens only for very small s ; for any significant s they are of approximately equal magnitude.

In Fig. 2 the same quantity is plotted as a function of filling, ρ , for fixed $s = 5t$. One can clearly see the optimal doping away from half filling at which T_c for fixed coupling will have a maximum. To illustrate the stabilizing effect of AF order, the inset in Fig. 2 shows the corresponding results for $s = 0$ (no AF order) for comparison. As expected, in this case the most stable SC occurs at half filling where the chemical potential intersects the van Hove singularity of the 2D DOS, but the required couplings g_{BCS} to reach significant T_c values are much larger than for finite s .

We also give some typical examples of T_c as a function of s , with the filling ρ fixed [Fig. 3(a)] and T_c as a function of ρ , with s fixed [Fig. 3(b)]. We only show the dominating mixed channels. Obviously the antiferromagnetic order can lead to critical temperatures compatible with experimental results for HTSC. Fig. 3(b) also shows that the maximum T_c occurs at a finite doping ($\rho \approx 0.9$ in the nn channel for the parameters considered), and T_c goes to zero as doping is decreased or increased away from that value, as observed in HTSC. For a more detailed comparison of the doping dependence of T_c with experiments on HTSC it is important to remember that $\rho - 1$ in our model accounts only for the doping of the AF bands. As discussed in Section II B, the latter is smaller than the

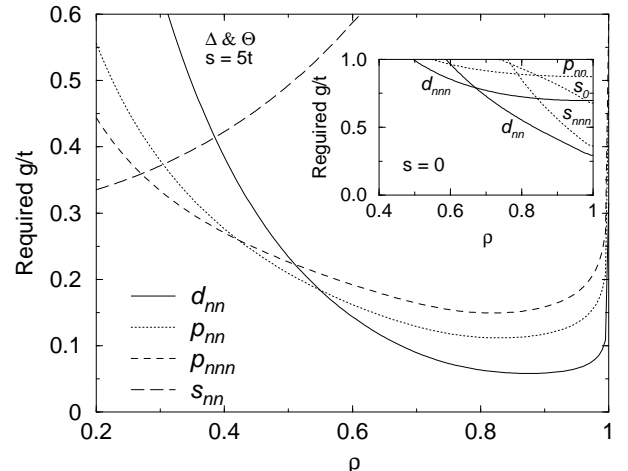


FIG. 2. Required coupling g_{BCS} to reach a critical temperature $T_c = 100\text{K}(t/1\text{eV})$ as a function of the filling ρ for fixed magnitude of the AF order, $s = 5t$. The different curves correspond to different shapes of the gap, for the mixed channels, $\Delta\&\Theta$. The purely translation invariant and staggered solutions require a much stronger coupling. The inset shows the corresponding result for $s = 0$ (no AF).

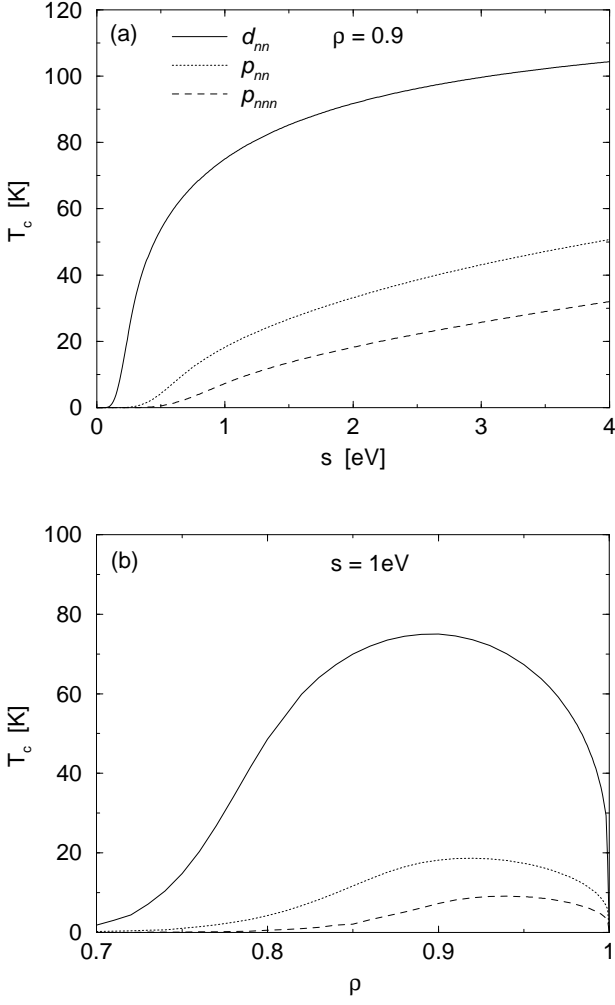


FIG. 3. Critical temperature T_c as a function of magnitude of antiferromagnetic order s and filling ρ , for dominating SC channel $\Delta\&\Theta$ and different shapes of the gap. Used parameters here are: $t = 0.5$ eV and $g_{BCS} = 0.05$ eV. (a) $\rho = 0.9$ fixed (b) $s = 1$ eV fixed. Labeling of results for different shapes of the gap as in Fig. 1.

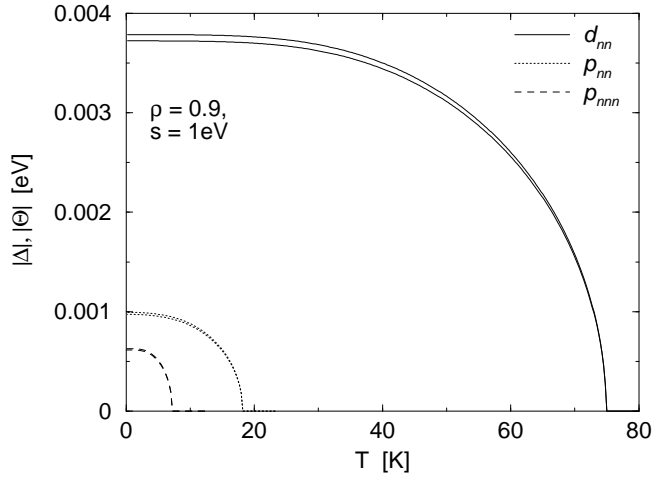


FIG. 4. Magnitude of the superconducting gaps, $|\Delta|$ and $|\Theta|$, as a function of temperature T for dominating channels $\Delta\&\Theta$. Two neighboring curves show the translation invariant (Δ) and staggered (Θ) parts of the gap. In all cases, $|\Delta|$ is slightly bigger than $|\Theta|$. Note that $|\Delta|$ and $|\Theta|$ are nearly the same, which shows that the SC gap closely follows the antiferromagnetic order, as discussed in the text (they become identical for $s \rightarrow \infty$). The parameters are $\rho = 0.9$, $s = 1$ eV, $t = 0.5$ eV and $g = 0.05$ eV.

total doping: part of the charge carriers are trapped in magnetic domain walls etc. not taken into account in our model.

We have also tested the validity of the BCS-like formulas $T_c = \Omega \exp(-1/g_{BCS}\Lambda)$. As discussed, one can expect this formula to be a good approximation for sufficiently small temperatures T_c , but we found that it works reasonably well up to quite high T_c values (for the parameters in Fig. 3(a) up to $T_c \approx 40$ K). Ω in this formula has the interpretation of an effective energy cut-off for the interaction, similar to the Debye frequency ω_D in the simple BCS model. It is interesting to note that for fixed ρ , Ω becomes independent of the shape of the gap for larger s -values. Moreover, Ω is comparable to the hopping constant t only for small s , but for larger s it goes like t^2/s and becomes much smaller than t . For the parameters adequate for high temperature superconductors which we considered here, Ω is huge — of order 1 eV $\approx 10^4$ K — for $s = 0$, but it becomes comparable to small values typical for standard superconductors (order 10 K) in presence of AF order. Nevertheless, without AF order ($s = 0$), one never can get a significant T_c since Λ is too small, and the increase of T_c with s is due to the increase of Λ resulting from the increase of the DOS in the AF bands, as discussed in the Introduction: Since Λ enters T_c exponentially, it overcompensates the decrease of Ω with s .

In Fig. 4 we show the temperature dependence of the magnitude of the superconducting order parameters Δ and Θ for parameters values realistic for HTSC

[Eqs. 4.28]. In all cases, $|\Delta|$ is slightly bigger than $|\Theta|$. Note that $|\Delta|$ and $|\Theta|$ are nearly the same, which shows that the SC gap closely follows the antiferromagnetic order. From this Fig. we also obtain $2|\Delta(T=0)|/k_B T_c \approx 1.17$, but we found that this parameter depends on doping and s and is not universal as in the BCS model. Note also that the SC gap here is \mathbf{k} -dependent, and one has to be very careful when comparing with results from experiments on HTSC (see below).

Another interesting quantity is the superconducting one-particle electronic density of states $N(\omega)$. In Fig. 5(a) we show how $N(\omega)$ changes as the temperature is lowered from T_c , for a d_{nn} -wave gap [Eq. (4.29)]. Here one sees how the SC gap opens up at the Fermi level, which is at $\omega = 0$. The filling used in the figure is chosen to give an optimal T_c for this value of s , and one clearly sees that the gap opens up precisely at the AF peak in $N(\omega)$ as the temperature is lowered below T_c . It is interesting that our simple model can lead to the rich structure in the DOS seen in the figure. In Fig. 5(b) we show the tunneling conductance, dI/dV , for a superconductor – normal-metal junction, which is essentially the same curve smeared out by positive temperature effects [Eq. (4.30)]. Here we note some significant features also seen in experiments [12]: (1) There is not a real gap but only a dip in the tunnel conductance. This is a consequence of the d -wave shape of the gap, which implies that it has nodes on the Fermi surface. (2) The positions of the two peaks do not move much as the temperature is lowered, even though they would be expected to, because of the increase of the gap. It is clear, especially when compared to Fig. 5(a), that this comes from thermal smearing. At low temperature, when the smearing is small, the gap is essentially constant as a function of temperature. Some details of the structure in the DOS remain visible at very low temperature. Note also that the separation of the two peaks is about $8|\Delta|$ (compare Figs. 4 and 5) and thus much bigger than the BCS prediction $2|\Delta|$ which is often used to fit experimental data. This shows that it can be misleading to apply BCS formulas naively to HTSC.

We conclude that for finite s , it is always the channel $\Delta \& \Theta_d^{nn}$ respectively $\Delta \& \Theta_p^{nnn}$ which is dominating: for a given coupling g_{nn} respectively g_{nnn} , it always leads to a T_c much bigger than the others, and also the gaps for the different channels remain well-separated for all temperatures. This justifies the simplified analysis neglecting mixing of different SC channels.

VI. CONCLUSION

In this paper we studied a simple model of coexisting superconductivity (SC) and antiferromagnetism (AF), and we developed flexible tools to study this and similar models. We also analyzed in detail the two dimensional version of this model which, as we argued, describes the

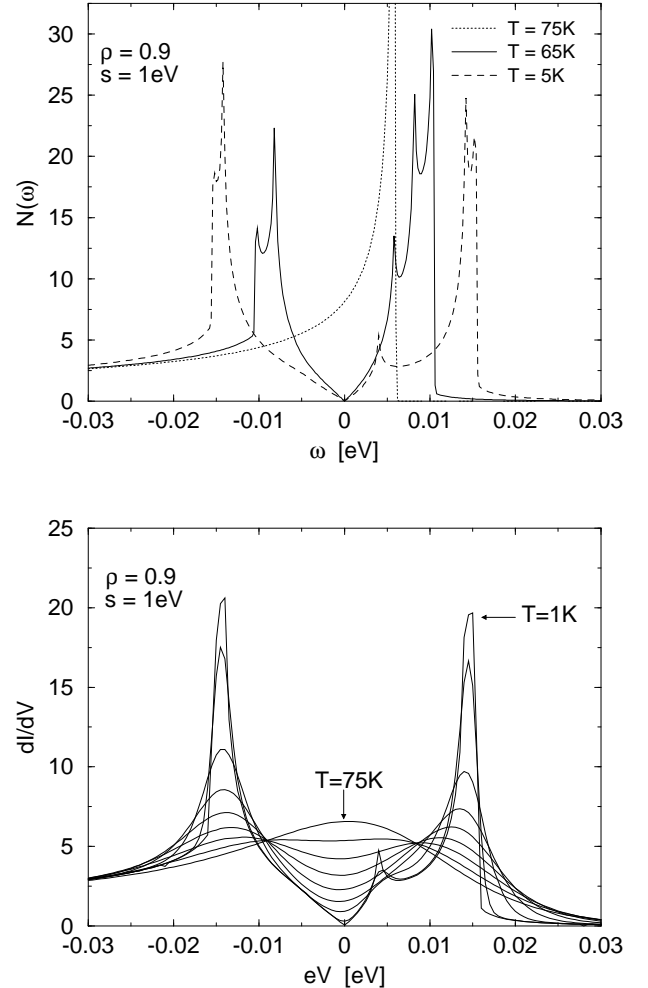


FIG. 5. (a) Superconducting density of states for three different temperatures $T = 75$ K, 65 K and 1 K. The parameters are the same as in Fig. 4, with a $T_c \approx 75$ K. The chemical potential is at $\omega = 0$. (b) Tunneling conductance dI/dV for a superconductor – normal-metal junction as a function of the applied voltage for a sequence of temperatures $T = 75, 65, 55, \dots, 5$ K and 1 K. Note that most of the fine structures in the density of states is washed out by temperature effects.

effect of AF on SC in HTSC. In case of nearest neighbor (nn) attraction, we found that the internal structure of the gap is d -wave, whereas for next-nearest neighbor (nnn) attraction it is p -wave. As soon as AF is present, the same coupling produces a much larger T_c in the d -wave than in the p -wave case, and on-site attraction leads only to insignificant T_c values. The most stable SC channels correspond to paired fermions pointing parallel to the AF order parameter, and in case the paired fermions are on adjacent sites (nn) these have opposite spins and correspond to a mixture of spin singlet and triplet. (The latter is possible because spin rotation symmetry is broken.) Our results give a detailed understanding of one particular effect which, as we believe, is important for superconductivity in correlated fermions systems: whenever AF correlations are present, peaks in the DOS will be enhanced, and in a certain filling regime the Fermi energy intersects such a peak which results in stable SC. It is important to note that the peak in the 2D DOS at half filling alone is not sufficient, but the enhancement of this peak by AF correlations is essential.

In contrast to models for conventional superconductors, the energy dependence of the gap is important in our model and cannot be neglected since the bands are very narrow. Thus our neglecting possible mixing of different channels is, *a priori*, an approximation: mixing of channels is prevented by symmetry only if the SC gap has a negligible energy dependence. Nevertheless, we could justify this approximation *a posteriori* by our numerical results.

As mentioned at the end of the Introduction, our results are on the magnitude of the SC order parameter and allow no predictions about its phase. It is interesting to see also formally how this comes about: In Section IV C we argued that for a HS configuration Eq. (4.24c), the HS action equals $\mathcal{F} = \beta L^d f_0$ with f_0 defined in Eq. (4.26). A more general boson configuration is of the form

$$\Delta(x) = |\Delta| e^{i\phi} e^{i\alpha(x)}, \quad \Theta(x) = |\Theta| e^{i\alpha(x)}, \quad (6.1)$$

and if the phase $\alpha(x)$ varies sufficiently little, the HS action of such a configuration is $\mathcal{F} = \beta L^d f_0 + \mathcal{F}_1$ with a correction \mathcal{F}_1 involving gradient terms in $\alpha(x)$. The latter can be made arbitrarily small if $\alpha(x)$ varies sufficiently little (i.e. it changes fast in a small fraction of the total spacetime volume and otherwise only has slow changes). Thus a minimum of f_0 accounts for the set of all states described by Eq. (6.1) where $\alpha(x)$ varies so little that $\lim_{L \rightarrow \infty} \mathcal{F}_1 / L^d \beta \approx 0$, and this set obviously contains states without long range order.

We finally would like to recall that the functional integral somewhat clarifies the physical meaning of mean field theory: the HS action Eq. (3.15) has the natural interpretation as free energy of a state represented by the HS configuration $\Delta(X, Y)$. Thus one can naturally interpret the exact path integral Eq. (3.1) as summation of free energy contributions over all states. The mean field theory done here is equivalent to restricting this summation to the small subset given in Eq. (4.1): if one sums

only over these states, the exact path integral reduces to a finite dimensional integral (we drop an irrelevant constant)

$$e^{-L^d \beta \Omega} = \int d\Delta d\Delta^* \int d\Theta d\Theta^* e^{-L^d \beta f_0(\Delta, \Theta)} \quad (6.2)$$

($\int d\Delta d\Delta^* \propto \int_{-\infty}^{\infty} d\text{Re}\Delta \int_{-\infty}^{\infty} d\text{Im}\Delta$ etc.), where $f_0 = f_0(\Delta, \Theta)$ is given by Eq. (4.26) and $\Omega = -\log(Z)/L^d \beta$ is the free energy density. Since we are interested in $L \rightarrow \infty$, the saddle point evaluation for this integral is exact, and we recover the mean field equations of Section IV C. Mean field theory can be improved by extending the class of configurations summed over. This can be done, e.g., by including Gaussian fluctuations around the saddle point.

In summary, we studied a simple model for lattice fermions in an external staggered magnetic field with a weak attractive interaction. This model gives a description at the mean field level of local antiferromagnetic correlations arising from the Coulomb repulsion in the Hubbard model, and this is thus useful e.g. for studying the role of antiferromagnetic correlations on superconducting properties in HTSC. We developed an efficient path integral formalism for studying this and similar models. Moreover, we presented a systematic study of T_c and the various different gap functions, and of the superconducting DOS and tunneling conductance. These quantities were then evaluated numerically for the 2D case. Our results show that high T_c and d -wave superconductivity comes naturally from a general treatment making a minimum of assumptions.

Acknowledgments. We thank Asle Sudbø for useful discussions. This work was supported by the Swedish Natural Science Research Council.

APPENDIX A: ON STAGGERED STATES

In this Appendix we show how to evaluate the inverse for Green functions etc. describing staggered states. Note that the quantities $A(x, y)$ etc. below are matrices and the matrix product is understood.

To get the inverse of $A(x, y) = A_N(x - y) + A_A(x - y)e^{iQy}$, we solve the equation

$$\sum_z (A_N(x - z) + A_A(x - z)e^{iQz}) \times (B_N(z - y) + B_A(z - y)e^{iQy}) = \delta_{x,y}, \quad (A1)$$

which, after Fourier transformation, can be written in a matrix form

$$\begin{pmatrix} A_N & A_A \\ A_A^Q & A_N^Q \end{pmatrix} \begin{pmatrix} B_N & B_A \\ B_A^Q & B_N^Q \end{pmatrix} = \begin{pmatrix} 1 & 0 \\ 0 & 1 \end{pmatrix} \quad (A2)$$

where $A_N^Q(k) = A_N(k - Q)$, etc. The solutions are (suppressing the argument k)

$$\begin{aligned} B_N &= (A_N - A_A(A_N^Q)^{-1}A_A^Q)^{-1} \\ B_A &= (A_A^Q - A_N^Q A_A^{-1} A_N)^{-1} \end{aligned} \quad (\text{A3})$$

If all of A_N, A_A, B_N, B_A commute,

$$\begin{aligned} B_N &= \frac{A_N^Q}{A_N A_N^Q - A_A A_A^Q} \\ B_A &= \frac{-A_A}{A_N A_N^Q - A_A A_A^Q} \end{aligned} \quad (\text{A4})$$

In particular, this gives the free Green function (4.5) as the inverse of $R = G_0^{-1}$, which from (3.3) has the translation invariant and staggered parts $R_{N,A}$ given in Eq. (4.22).

APPENDIX B: T_c EQUATIONS

Here we give some details of our derivation of the T_c equation in Section IV B.

We use the following notation for functions of k :

$$f^Q(k) = f(k - Q), \quad \tilde{f}(k) = -f(-k)$$

We also write $G_N(k) = g(k)\sigma_0$, $G_A(k) = a(k)\sigma_3$ and use that $\eta^Q(k) = \eta(k - Q) = p\eta(k)$, where $p = \pm 1$ depending on the parity of $\Delta(k)$.

With that we obtain the equations

$$\begin{aligned} \Delta_{1,4} &= -g_{BCS} \sum_k \left((g\tilde{g}\eta^2 + a\tilde{a}^Q\eta\eta^Q) \Delta_{1,4} \right. \\ &\quad \left. \pm (g\tilde{a}^Q\eta^2 + a\tilde{g}\eta\eta^Q) \Theta_{1,4} \right) \\ \Theta_{1,4} &= -g_{BCS} \sum_k \left((g\tilde{g}^Q\eta^2 + a\tilde{a}\eta\eta^Q) \Theta_{1,4} \right. \\ &\quad \left. \pm (g\tilde{a}\eta + a\tilde{g}^Q\eta\eta^Q) \Delta_{1,4} \right) \end{aligned}$$

and

$$\begin{aligned} \Delta_{2,3} &= -g_{BCS} \sum_k \left((g\tilde{g}\eta^2 - a\tilde{a}^Q\eta\eta^Q) \Delta_{2,3} \right. \\ &\quad \left. \mp (g\tilde{a}^Q\eta^2 - a\tilde{g}\eta\eta^Q) \Theta_{2,3} \right) \\ \Theta_{2,3} &= -g_{BCS} \sum_k \left((g\tilde{g}^Q\eta^2 - a\tilde{a}\eta\eta^Q) \Theta_{2,3} \right. \\ &\quad \left. \mp (g\tilde{a}\eta^2 - a\tilde{g}^Q\eta\eta^Q) \Delta_{2,3} \right) \end{aligned}$$

Doing the Matsubara sums and defining

$$\chi_\beta(E) \equiv \frac{1}{\beta} \sum_{\omega_n} \frac{1}{\omega_n^2 + E^2} = \frac{\tanh(\beta E/2)}{2E} \quad (\text{B1})$$

results in Eq. (4.13) with the constants

$$\begin{aligned} K_+(\beta) &= \int d\mathbf{k} \left(\frac{1}{2} (\chi_\beta(E_+) + \chi_\beta(E_-)) \eta_J^2 \right) \\ K_-(\beta) &= \int d\mathbf{k} \left(\frac{1}{2} (\chi_\beta(E_+) + \chi_\beta(E_-)) \eta_J^2 \right. \\ &\quad \left. - \frac{s^2}{2\mu w} (\chi_\beta(E_+) - \chi_\beta(E_-)) \eta_J^2 \right) \\ \tilde{K}_+(\beta) &= \int d\mathbf{k} \left(\frac{1}{2} (\chi_\beta(E_+) + \chi_\beta(E_-)) \eta_J^2 \right. \\ &\quad \left. - \frac{\epsilon^2}{2\mu w} (\chi_\beta(E_+) - \chi_\beta(E_-)) \eta_J^2 \right) \\ \tilde{K}_-(\beta) &= \int d\mathbf{k} \left(\frac{1}{2} (\chi_\beta(E_+) + \chi_\beta(E_-)) \eta_J^2 \right. \\ &\quad \left. - \frac{w}{2\mu} (\chi_\beta(E_+) - \chi_\beta(E_-)) \eta_J^2 \right) \\ L_+(\beta) &= \int d\mathbf{k} \left(\frac{s}{2w} (\chi_\beta(E_+) - \chi_\beta(E_-)) \eta_J^2 \right) \\ L_-(\beta) &= 0 \end{aligned} \quad (\text{B2})$$

where $w = \sqrt{\epsilon^2 + s^2}$ and $E_\pm = -\mu \pm w$. Note that all these expressions have well-defined limits $\mu \rightarrow 0$.

It is shown below (and can be checked numerically) that the β dependence of these integrals for large β is in a very good approximation given by (these formulas becomes exact for $\beta \rightarrow \infty$)

$$\begin{aligned} K_+(\beta) &= M \log(\Omega^{(a)}\beta), \quad K_-(\beta) = \tilde{\alpha} \\ \tilde{K}_+(\beta) &= \frac{s^2}{\mu^2} M \log(\Omega^{(b)}\beta) + \alpha, \quad \tilde{K}_-(\beta) = \alpha + \tilde{\alpha} \quad (\text{B3}) \\ L_+(\beta) &= \frac{s}{\mu} M \log(\Omega^{(c)}\beta) \end{aligned}$$

with M Eq. (4.17) and $\alpha = \alpha_\beta$ and $\tilde{\alpha} = \tilde{\alpha}_\beta$ are, in a very good approximation, independent of β for large β [the latter can be checked numerically; the energy scales $\Omega^{(a,b,c)}$ can be obtained by calculating the integrals $K_+(\beta)$ etc. for one (large) β -value numerically and comparing with (B3).] This yields the T_c -equations of the form Eq. (4.18).

The step going from (B2) to (B3) uses that functions $F(E)$ reasonably smooth close to $E = 0$, the β -dependence of

$$I(F, \beta) = \int dE F(E) \frac{\tanh(\beta E/2)}{2E} \quad (\text{B4})$$

for large β is approximated well by

$$I(F, \beta) = F(0) \log(\Omega_F \beta) \quad (\text{B5})$$

To see this, define

$$\Omega(F, \beta) = \frac{1}{\beta} e^{I(F, \beta)/F(0)},$$

then $I(F, \beta) = F(0) \log(\Omega(F, \beta)\beta)$. Now, with $x = \beta E/2$,

$$\frac{d\Omega}{d\beta} = \frac{\Omega}{\beta} \left(\int dx \frac{F(2x/\beta)}{F(0)} \frac{1}{2 \cosh^2(x)} - 1 \right)$$

Taylor expanding F , we see that $d\Omega/d\beta = O(1/\beta^3)$ so we can replace $\Omega(F, \beta)$ by $\Omega_F = \lim_{\beta \rightarrow \infty} \Omega(F, \beta)$ up to terms of order $1/\beta^2$.

Fourier analysis on the entire Brillouin zone and keep track of translational symmetry breaking by the additional index $\in \{N, A\}$.

- [1] E. Dagotto, *Rev. Mod. Phys.* **66**, 763 (1994)
- [2] see e.g. M. Inui and P.H. Littlewood, *Phys. Rev. B* **44**, 4415 (1991); J.A. Vergés et.al, *Phys. Rev. B* **43**, 6099 (1991)
- [3] see e.g. S-W. Cheong *et.al.*, *Phys. Rev. Lett.* **67**, 1791 (1991); J.M. Tranquada *et.al.*, *Phys. Rev. Lett.* **64**, 800 (1990); G. Shirane *et.al.*, *Phys. Rev. Lett.* **63**, 330 (1989)
- [4] P. Monthoux and D. Pines, *Phys. Rev. B* **49**, 4261 (1994); K. Ueda, T. Moriya, and Y. Takahashi, *J. Phys. Chem. Solids* **53**, 1515 (1992); N.E. Bickers, D.J. Scalapino, S.R. White, *Phys. Rev. Lett.* **62**, 961 (1989)
- [5] J.R. Schrieffer, X.G. Wen, and S.C. Zhang, *Phys. Rev. B* **39**, 11663 (1989); G. Vignale and K.S. Singwi, *Phys. Rev. B* **39**, 2956 (1989); Z.Y. Weng, T.K. Lee, and S.C. Ting, *Phys. Rev. B* **38**, 6561 (1988)
- [6] E. Dagotto, A. Nazarenko and A. Moreo, *Phys. Rev. Lett.* **74**, 310 (1995); A. Nazarenko and E. Dagotto, [cond-mat/9510030](#); A. Nazarenko, S. Haas, J. Riera, A. Moreo, E. Dagotto, [cond-mat/9603046](#)
- [7] for review see D.J. Scalapino, *Phys. Rep.* **250**, 329 (1995)
- [8] for review see e.g. Chapter 10 in: A.C. Hewson, *The Kondo Problem to Heavy Fermions*, Cambridge Studies in Magnetism (Cambridge University Press, 1993)
- [9] T.E. Grigereit et al., *Phys. Rev. Lett.* **73** (1994) 2756
- [10] Kleinert H., *Fortschr. der Physik* **26**, 565 (1978)
- [11] E. Langmann and M. Wallin, to be published
- [12] T. Hasegawa, H. Ikuta, and K. Kitazawa in: D.M. Ginsberg (editor), *Physical properties of high temperature superconductors*, World Scientific Vol.III (1992), p. 526
- [13] M. Kato and K. Machida, *Phys. Rev. B* **37**, 1510 (1988)
- [14] K. Machida in: A. Narlikar (editor), *Studies of high temperature superconductors* Vol. 1, Nova Science Publishers (New York, 1989)
- [15] see e.g. C.C. Tsuei, D.M. Newns, C.C. Chi, P.C. Pattnaik, *Phys. Rev. Lett.* **65**, 2724 (1990)
- [16] See e.g. H.J. Schulz, *Phys. Rev. Lett.* **65**, 2462 (1990). Our notation here follows Ref. [11].
- [17] see the discussion in the third reference of [6]
- [18] N. Bulut, [cond-mat/9606204](#), especially Fig. 7
- [19] see e.g. Negele J.W. and Orland H., *Quantum many-particle systems*, Frontiers in Physics, Addison-Wesley (1988); note that our conventions for the Green functions are such that $\mathcal{G}(X, Y) = -\langle T_\tau \Psi(X) \Psi^\dagger(Y) \rangle$ (T_τ imaginary-time ordering) and differ from the ones used in this book by a sign
- [20] We write such functions in terms of two translational invariant ones, $X(x, y) = X_N(x - y) + X_A(x - y)e^{i\mathbf{Q} \cdot \mathbf{y}}$. The advantage of this is that we then can use the usual